

Quantum geometric tensor and the topological characterization of the extended Su-Schrieffer-Heeger model

Xiang-Long Zeng(曾相龙), Wen-Xi Lai(赖文喜), Yi-Wen Wei(魏祎雯), and Yu-Quan Ma(马余全)

Citation: Chin. Phys. B, 2024, 33 (**3**): 030310. DOI: 10.1088/1674-1056/ad1170
Journal homepage: http://cpb.iphy.ac.cn; http://iopscience.iop.org/cpb

What follows is a list of articles you may be interested in

Hall conductance of a non-Hermitian two-band system with *k*-dependent decay rates

Junjie Wang(王俊杰), Fude Li(李福德), and Xuexi Yi(衣学喜)
Chin. Phys. B, 2023, 32 (**2**): 020305. DOI: 10.1088/1674-1056/ac9046

Topological superconductivity in Janus monolayer transition metal dichalcogenides

Xian-Dong Li(李现东), Zuo-Dong Yu(余作东), Wei-Peng Chen(陈伟鹏), and Chang-De Gong(龚昌德)
Chin. Phys. B, 2022, 31 (**11**): 110304. DOI: 10.1088/1674-1056/ac8739

Non-Hermitian Weyl semimetals: Non-Hermitian skin effect and non-Bloch bulk-boundary correspondence

Xiaosen Yang(杨孝森), Yang Cao(曹阳), and Yunjia Zhai(翟云佳)
Chin. Phys. B, 2022, 31 (**1**): 010308. DOI: 10.1088/1674-1056/ac3738

Photoinduced Weyl semimetal phase and anomalous Hall effect in a three-dimensional topological insulator

Meng-Nan Chen(陈梦南) and Wen-Chao Chen(陈文潮)
Chin. Phys. B, 2021, 30 (**11**): 110308. DOI: 10.1088/1674-1056/abff29

Geometry of time-dependent $\mathcal{PT}$-symmetric quantum mechanics

Da-Jian Zhang(张大剑), Qing-hai Wang(王清海), and Jiangbin Gong(龚江滨)
Chin. Phys. B, 2021, 30 (**10**): 100307. DOI: 10.1088/1674-1056/ac0ba8

Quantum geometric tensor and the topological characterization of the extended Su–Schrieffer–Heeger model

Xiang-Long Zeng(曾相龙), Wen-Xi Lai(赖文喜), Yi-Wen Wei(魏祎雯), and Yu-Quan Ma(马余全)†

School of Science, Beijing Information Science and Technology University, Beijing 100192, *China*

(Received 16 July 2023; revised manuscript received 20 October 2023; accepted manuscript online 1 December 2023)

We investigate the quantum metric and topological Euler number in a cyclically modulated Su–Schrieffer–Heeger (SSH) model with long-range hopping terms. By computing the quantum geometry tensor, we derive exact expressions for the quantum metric and Berry curvature of the energy band electrons, and we obtain the phase diagram of the model marked by the first Chern number. Furthermore, we also obtain the topological Euler number of the energy band based on the Gauss–Bonnet theorem on the topological characterization of the closed Bloch states manifold in the first Brillouin zone. However, some regions where the Berry curvature is identically zero in the first Brillouin zone result in the degeneracy of the quantum metric, which leads to ill-defined non-integer topological Euler numbers. Nevertheless, the non-integer "Euler number" provides valuable insights and an upper bound for the absolute values of the Chern numbers.

Keywords: quantum geometric tensor, topological Euler number, Chern number, Berry curvature, quantum metric, Su–Schrieffer–Heeger (SSH) model

PACS: 03.65.Vf, 73.43.Nq, 75.10.Pq, 05.70.Jk **DOI:** 10.1088/1674-1056/ad1170

1. Introduction

The Su–Schrieffer–Heeger (SSH) model is a topological quantum system model with a simple structure, but distinct topological properties.[1–6] These include a winding number that characterizes the topological properties and the correspondence between bulk and edge states.[7–11] In addition, SSH models can be used to describe one-dimensional polyacetylene, graphene ribbons, p-orbital light ladder systems[12,13] and off-diagonal two-color optical lattices.[14] Historically, the Haldane model introduced a next-nearest neighbor (NNN) interaction into a two-dimensional honeycomb structure to realize the anomalous quantum Hall effect.[9] This caused the system to undergo a topological phase transition from an ordinary insulator to a Chern insulator. Interestingly, if we expand the SSH model by adding appropriate cyclic modulation parameters, we can obtain a phase diagram similar to the two-dimensional Haldane model,[15] which further enriches the theoretical value of the one-dimensional SSH model and can be used to simulate two-dimensional topological systems.[16–20] The parameters of the modulated SSH model can be obtained through existing experimental techniques involving cold atoms, optical setups or waveguide systems,[21–24] such as the interaction of fermion atoms on a two-legged ladder.[13] These results can be verified by using existing experiments.

As a general covariant tensor in Hilbert space geometry, the quantum geometric tensor (QGT) $Q_{\mu\nu} = g_{\mu\nu} - \frac{\mathrm{i}}{2}F_{\mu\nu}$[25,26] defined on a parameterized quantum state manifold is expected to shed some light on the quantum phase transitions in many-body systems.[27–29] Its imaginary part (up to a coefficient) corresponds to the Berry curvature, which is a key quantity to derive the first Chern number in order to understand the topological aspects of quantum matter. Especially, the quantum metric (real part of the QGT) proposed by Provost and Valee[25] is a positive semi-definite Riemannian metric, which defines a gauge-invariant distance between two adjacent quantum states in a parameterized Hilbert space. Recently, it was shown that the quantum metric plays a crucial role in quantum transport phenomena, quantum noise, optical conductivity, the anomalous Hall effect, unconventional superconductivity and related topics.[30–57] Furthermore, it has been revealed that the quantum metric can provide a topological Euler number for the energy band. This is based on the Gauss–Bonnet theorem applied to the topological characterization of the closed Bloch state manifold in the first Brillouin zone, which provides an effective topological index for a class of nontrivial topological phases.[58–72]

This paper is structured as follows. In Section 2, we study a cyclically modulated SSH model with long-range hopping terms and solve its Hamiltonian in the Bloch momentum space with periodic conditions. In Section 3, we obtain the QGT for the occupied lower band of the extended SSH model. The critical points in the model can be witnessed by the singularity behaviors of the Berry curvature and the quantum metric. In Section 4, we study the topological Euler number of this model and compare the phase diagrams marked by the Chern and Euler numbers, respectively. Finally, we provide a summary of our work.

†Corresponding author. E-mail:abelish@163.com

© 2024 Chinese Physical Society and IOP Publishing Ltd

2. The model

We consider the SSH model with N lattice points, the Hamiltonian can be written as[6]

$$H = \sum_{j=1}^{N} (t_1 \hat{a}_j^\dagger \hat{b}_j + t_2 \hat{b}_j^\dagger \hat{a}_{j+1} + t_3 \hat{a}_j^\dagger \hat{b}_{j+1} + t_A \hat{a}_j^\dagger \hat{a}_{j+1} + t_B \hat{b}_j^\dagger \hat{b}_{j+1} + \text{H.c.}), \quad (1)$$

where $\hat{a}_j^\dagger$ ($\hat{a}_j$) and $\hat{b}_j^\dagger$ ($\hat{b}_j$) are the creation (annihilation) operators at sublattices A and B for each j-th cell, t_1, t_2 and t_3 represent the nearest-neighbor (NN), NNN and third-nearest-neighbor (TNN) hopping amplitudes (see Fig. 1).

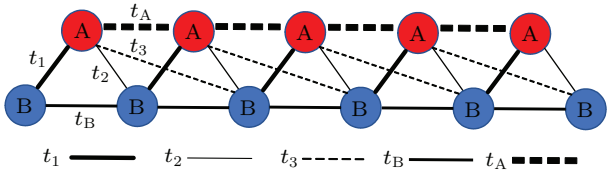


Fig. 1. The extended SSH model of long-range interactions.

Now, we modulate t_1 and t_2 as

$$t_1 = 1 + \frac{1}{2}\cos\theta, \quad t_2 = 1 + \frac{1}{2}\cos\theta, \quad (2)$$

with θ representing a cyclical parameter varying from 0 to 2π. Meanwhile, t_A and t_B are modulated as

$$t_A = h + \cos(\theta + \phi), \quad t_B = h + \cos(\theta - \phi), \quad (3)$$

where ϕ is an additional parameter used to adjust the strength relation between t_A and t_B. Then we consider the periodic boundary conditions and introduce the following Fourier transformation:

$$\hat{a}_k = \frac{1}{\sqrt{N}} \sum_j e^{ikj} \hat{a}_j, \quad \hat{b}_k = \frac{1}{\sqrt{N}} \sum_j e^{ikj} \hat{b}_j, \quad (4)$$

and the Hamiltonian in momentum space can be written as

$$H = \sum_k (\hat{a}_k^\dagger, \hat{b}_k^\dagger) h(k,\theta) \begin{pmatrix} \hat{a}_k \\ \hat{b}_k \end{pmatrix}, \quad (5)$$

where

$$h(k,\theta) = \begin{pmatrix} 2t_A \cos k & t_1 + t_2 e^{-ik} + t_3 e^{ik} \\ t_1 + t_2 e^{ik} + t_3 e^{-ik} & 2t_B \cos k \end{pmatrix}. \quad (6)$$

The $h(k,\theta)$ can be written in the form of Pauli matrices

$$h(k,\theta) = \varepsilon(k,\theta) I_{2\times 2} + \sum_{\alpha=1}^{3} d_\alpha(k,\theta) \cdot \sigma_\alpha, \quad (7)$$

where $\varepsilon(k,\theta)$ is the eigenvalue of the Hamiltonian, $I_{2\times 2}$ is a 2×2 identity matrix, $d_\alpha(k,\theta)$ is the coefficient of the Pauli matrix and σ_α is a Pauli matrix, representing pseudo-spin degrees of freedom. The diagonalization of $h(k,\theta)$ is straightforward and the eigenvalues can be written as

$$E(k,\theta) = \varepsilon(k,\theta) \pm \sqrt{\sum_{\alpha=1}^{3} d_\alpha^2(k,\theta)}, \quad (8)$$

and the eigenvectors are

$$u(k,\theta) = \frac{1}{\sqrt{2d(d \mp d_3)}} \begin{pmatrix} d_1 - i d_2 \\ \pm d - d_3 \end{pmatrix}. \quad (9)$$

Here we choose the following modulated extended SSH model of long-range interactions as an example because it has richer topological properties and a higher Chern number topological phase than the ordinary SSH model. In this model, the Hamiltonian of the Bloch state momentum space is

$$\begin{aligned} \varepsilon(k,\theta) &= (2h + 2\cos\theta\cos\varphi)\cos k, \\ d_1 &= (1 + \frac{1}{2}\cos\theta) + (1 - \frac{1}{2}\cos\theta + t_3)\cos k, \\ d_2 &= (1 - \frac{1}{2}\cos\theta - t_3)\sin k, \\ d_3 &= (2h - 2\sin\varphi\sin\theta)\cos k. \end{aligned} \quad (10)$$

It is obvious that the model is a generalized topological system. When $t_3 = t_A = t_B = 0$, and $t_1 \neq 0$, $t_2 \neq 0$, or when $t_1(t_2) = t_A = t_B = 0$ and $t_2(t_1) \neq 0$, the system will degenerate into a one-dimensional SSH model, but when $t_3 = 0$ and $t_A, t_B \neq 0$, the system will become an extended SSH model of NNN interactions. Obviously, for $t_A = t_B = 0$ and $t_1, t_2, t_3 \neq 0$, the model is equal to the two-coupled SSH models.

3. Quantum metric, Berry curvature and the quantum geometric tensor

Firstly, we introduce the QGT in the Bloch momentum space. It is derived from the gauge-invariant metric between two states on the $U(1)$ line bundle. We consider two close wave functions in the parameterized Hilbert space $|\varphi(k)\rangle$ and $|\varphi(k+\delta k)\rangle$, where $k = (\mu, \nu)$ denotes the Hamiltonian parameters (k,θ) for convenience. The distance between two close wave functions is given by

$$dS^2 = \langle \partial_\mu \varphi(k) d\mu | \partial_\nu \varphi(k) d\nu \rangle, \quad (11)$$

extending the factor $|\partial_\mu \varphi(k) d\mu\rangle$ to

$$|\partial_\mu \varphi(k) d\mu\rangle = |D_\mu \varphi(k)\rangle + [1 - P(k)] |\partial_\mu \varphi(k)\rangle, \quad (12)$$

where $P(k) = |\varphi(k)\rangle\langle\varphi(k)|$ is the projection operator and $|D_\mu \varphi(k)\rangle = P(k)|\partial_\mu \varphi(k)\rangle$ is the covariant derivative of $|\varphi(k)\rangle$. The quantum adiabatic approximation guarantees the parallel transport of the evolution of $|\varphi(k)\rangle$ to $|\varphi(k+\delta k)\rangle$ on the $U(1)$ line bundle; therefore, $|D_\mu \varphi(k)\rangle = 0$. We substitute Eq. (11) into Eq. (12) to obtain the quantum metric

$$dS^2 = \langle \partial_\mu \varphi(k)| [1 - P(k)] |\partial_\nu \varphi(k)\rangle d\mu d\nu. \quad (13)$$

In addition, the QGT is

$$Q_{\mu\nu} = \langle \partial_\mu \varphi(k)| [1 - P(k)] |\partial_\nu \varphi(k)\rangle, \quad (14)$$

separating the QGT into real and imaginary parts. We know that the real part is the quantum metric $g_{\mu\nu} = \mathrm{Re}Q_{\mu\nu}$ and the imaginary part is $1/2$ of the negative value of the Berry curvature as $F_{\mu\nu} = -2\mathrm{Im}Q_{\mu\nu}$. Thus we get the QGT for $Q_{\mu\nu} = g_{\mu\nu} - \frac{\mathrm{i}}{2}F_{\mu\nu}$. Its imaginary part is canceled in the summation of the distance due to its antisymmetric nature; then, the quantum metric can be rewritten as $\mathrm{d}S^2 = \sum_{\mu\nu}\mathrm{Re}Q_{\mu\nu}\mathrm{d}\mu\,\mathrm{d}\nu$. Given that $P(k) = |\varphi(k)\rangle\langle\varphi(k)|$, we substitute it into Eq. (14) to get the QGT

$$Q_{\mu\nu} = \langle\partial_\mu\varphi(k)|\,[1 - |\varphi(k)\rangle\langle\varphi(k)|]\,|\partial_\nu\varphi(k)\rangle\,. \tag{15}$$

Substituting Eq. (15) into $F_{\mu\nu} = -2\mathrm{Im}Q_{\mu\nu}$ gives

$$F_{\mu\nu} = \langle\partial_\mu\varphi(k)|\partial_\nu\varphi(k)\rangle - \langle\partial_\nu\varphi(k)|\partial_\mu\varphi(k)\rangle\,, \tag{16}$$

then the Berry curvature can be calculated by Eqs. (16) and (9)

$$F_{\mu\nu} = \frac{1}{2}[\hat{\boldsymbol{d}}\cdot\partial_\mu\hat{\boldsymbol{d}}\times\partial_\nu\hat{\boldsymbol{d}}], \tag{17}$$

where $\hat{\boldsymbol{d}}$ represents the unit vector $\boldsymbol{d}/d$ (see Appendix A for details). We calculate $g_{\mu\nu} = \mathrm{Re}Q_{\mu\nu}$ according to Eq. (15)

$$g_{\mu\nu} = \frac{1}{2}\langle\partial_\mu\varphi(k)|\partial_\nu\varphi(k)\rangle + \frac{1}{2}\langle\partial_\nu\varphi(k)|\partial_\mu\varphi(k)\rangle - \langle\partial_\mu\varphi(k)|\varphi(k)\rangle\langle\varphi(k)|\partial_\nu\varphi(k)\rangle\,. \tag{18}$$

The direct calculations of quantum metric $g_{\mu\nu}$ are tedious; however, it can be verified that there is a simple relation between the quantum metric determinant and the Bloch state $|\varphi(k)\rangle$ (for details see the Appendix A in Ref. [57]):

$$\sqrt{\det(g_{\mu\nu})} = \sqrt{(\hat{\boldsymbol{d}}\cdot\partial_\mu\hat{\boldsymbol{d}}\times\partial_\nu\hat{\boldsymbol{d}})^2/4}. \tag{19}$$

We can get the relationship between quantum metric and Berry curvature by comparing Eqs. (17) and (19)

$$\det g_{\mu\nu} = \frac{1}{4}(F_{\mu\nu})^2. \tag{20}$$

In Fig. 2, we show the determinant of the quantum metric $\det g_{\mu\nu}$ and Berry curvature $F_{\mu\nu}$ as functions of quasi-momentum θ, k in the first Brillouin zone, with different modulation parameters.

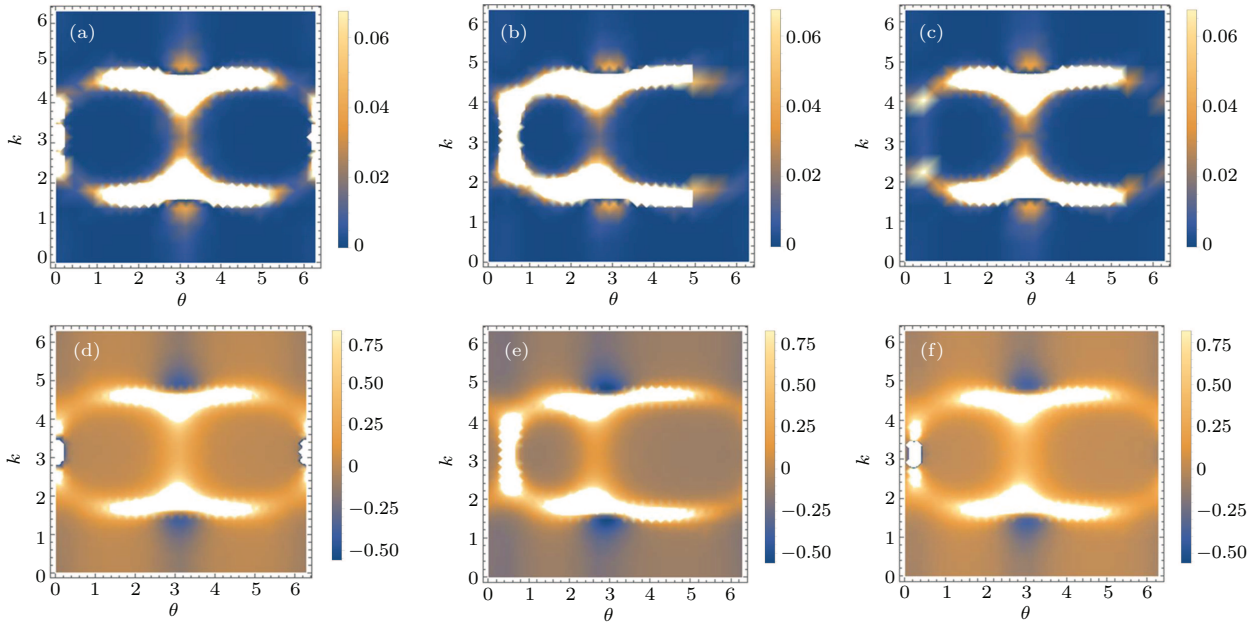


Fig. 2. The determinant of the quantum metric $\det g_{\mu\nu}$ and Berry curvature $F_{\mu\nu}$ as the functions of quasi-momentum θ, k in the first Brillouin zone, with different modulation parameters. (a) $\det g_{\mu\nu}$ with $h = 0.2$, $\phi = \pi/2$, $t_3 = 0.9$. (b) $F_{\mu\nu}$ with $h = 0.2$, $\phi = \pi/2$, $t_3 = 0.9$. (c) $\det g_{\mu\nu}$ with $h = 1$, $\phi = \pi/2$, $t_3 = 1$. (d) $F_{\mu\nu}$ with $h = 1$, $\phi = \pi/2$, $t_3 = 1$. (e) $\det g_{\mu\nu}$ with $h = 0.5$, $\phi = \pi/2$, $t_3 = 0.9$. (f) $F_{\mu\nu}$ with $h = 0.5$, $\phi = \pi/2$, $t_3 = 0.9$.

4. Topological Euler number

In the two-dimensional parameter $(\mu, \nu) := (k, \theta)$ space, the topology of the first Brillouin zone is a two-dimensional torus. Considering the Hamiltonian in the two-dimensional momentum space, the Bloch state $|\varphi(k)\rangle$ will adiabatically evolve a $U(1)$ line bundle. The first Chern number, which serves as a topological invariant for all filled bands, can be obtained by integrating the imaginary part (Berry curvature) of the QGT over the Brillouin zone

$$C = \frac{1}{2\pi}\sum_n\iint_{\mathrm{BZ}}F_{\mu\nu}\mathrm{d}\mu\,\mathrm{d}\nu. \tag{21}$$

Here, we assume that the model is half-filled and substitute Eq. (17) into Eq. (21)

$$C = \frac{1}{4\pi}\iint(\hat{\boldsymbol{d}}\cdot\partial_\mu\hat{\boldsymbol{d}}\times\partial_\nu\hat{\boldsymbol{d}})\,\mathrm{d}\mu\,\mathrm{d}\nu. \tag{22}$$

As shown in Fig. 3, the model can exhibit different topological phases with higher Chern numbers by varying the NNN

hopping term and it undergoes the corresponding topological quantum phase transitions.

The topological Euler numbers can be derived from the Gauss–Bonnet theorem based on the quantum metric (real part of the QGT)

$$\chi = \frac{1}{2\pi}\int_{\mathrm{BZ}} \kappa \mathrm{d}A, \tag{23}$$

where $\kappa = R_{\mu\nu\mu\nu}/\det g$ is the Gauss curvature and $\mathrm{d}A = (\det g)^{1/2}\mathrm{d}\mu\,\mathrm{d}\nu$ denotes the measured area according to the metric g and $R_{\mu\nu\mu\nu}$ is the covariant Riemannian curvature tensor. The direct calculation of the Gauss curvature is complicated, but it can be verified that there exists the following relation (for details see Appendix B in Ref. [57]) in a generalized two-band Hamiltonian on a 2D manifold as $R_{\mu\nu\mu\nu} = 4\det g$. Then, we generalize Eq. (23) to get the topological Euler number with an energy band in the first Brillouin zone

$$\chi = \frac{2}{\pi}\int_{\mathrm{BZ}} \sqrt{\det g}\,\mathrm{d}\mu\,\mathrm{d}\nu. \tag{24}$$

The results for the topological Euler numbers are shown in Fig. 4 with the Hamiltonian of parameters $t_3 = 1$, $h = 1/2$.

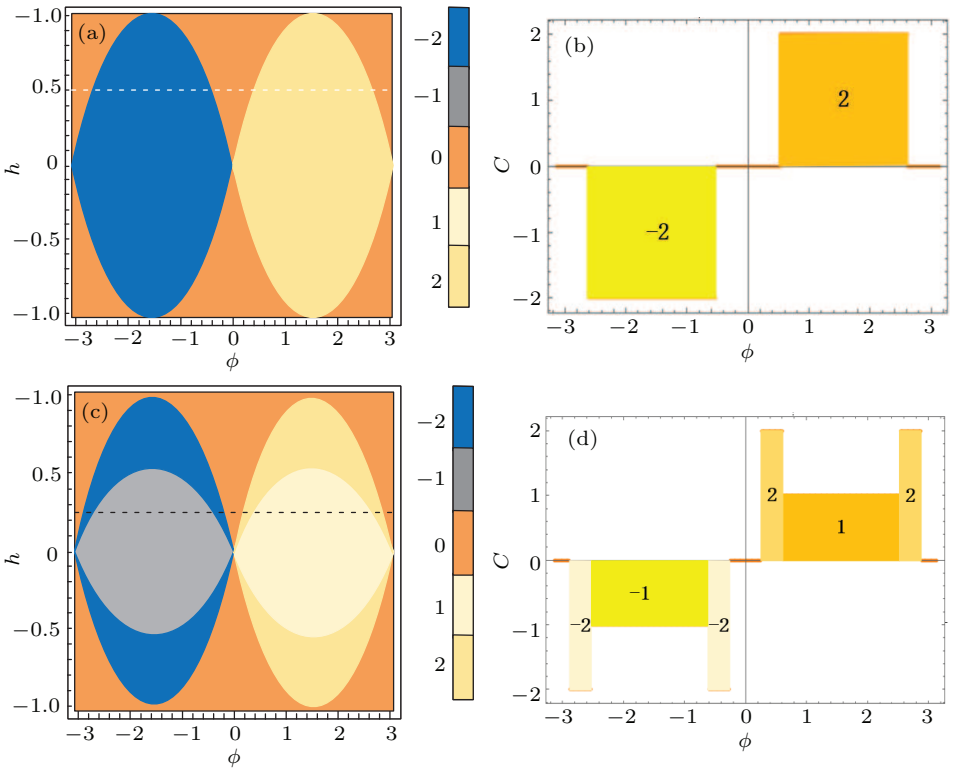


Fig. 3. The Chern number varies with the parameters h and ϕ, and the other parameters are set to (a) $t_3 = 1$. (b) The Chern number for the white line in (a) where $h = 1/2$ with $\phi \in (-3, 3)$. (c) $t_3 = 0.9$. (d) The Chern number for the white line in (a) where $h = 1/4$ with $\phi \in (-3, 3)$.

As shown in Fig. 4, the Euler number of the lower energy band is not exactly equal to 4 in the topological nontrivial phase where the first Chern number $= \pm 2$. The reason for this is that the quantum metric tensor is actually positive semi-definite. In a general two-dimensional two-band system, it can be proven that (for more details see Ref. [73]): (1) If the phase is topologically trivial, then the quantum metric must be degenerate — $\det(g) = 0$ in some region of the first Brillouin zone. This leads to the invalidity of the Gauss–Bonnet formula and exhibits an ill-defined "non-integer Euler number". (2) If the phase is topological nontrivial with a non-vanishing Berry curvature, then the quantum metric will be a positive definite Riemann metric in the entire first Brillouin zone. Therefore, the Euler number of the energy band is guaranteed to be an even number $2(1-g)$ by the Gauss–Bonnet theorem on the closed two-dimensional Bloch energy band manifold with the genus g, which provides an effective topological index for a class of nontrivial topological phases.

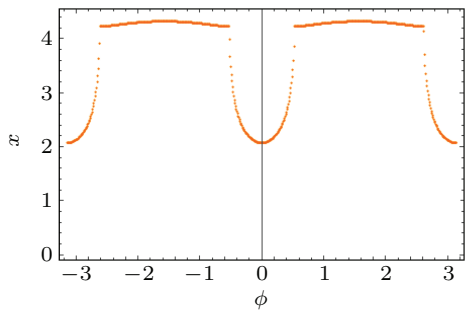


Fig. 4. The Euler number varies with the parameter ϕ and the other parameters are set to $t_3 = 1$, $h = 1/2$.

5. Conclusion

In summary, we study the QGT and topological Euler number of an extended SSH model with long-range hopping

terms. We show that the phase boundaries of the model can be witnessed by the singularity behaviors of both the Berry curvature and the quantum metric. We also study the topological Euler number of this model and make a comparison between the phase diagrams marked by the Chern and Euler numbers, respectively. The degeneracy of the quantum metric in some regions of the first Brillouin zone leads to non-integer Euler numbers. However, the non-integer Euler number can also provide an upper bound for the corresponding Chern numbers.[73]

Appendix A

Here, we provide the details for the calculation of Berry curvature $F_{\mu\nu}=\frac{1}{2}[\hat{\boldsymbol{d}}\cdot\partial_\mu\hat{\boldsymbol{d}}\times\partial_\nu\hat{\boldsymbol{d}}]$. For a modulated extended SSH model of long-range interactions in the 2D quasi-momentum space, the Bloch Hamiltonian can be written as $h(k,\theta)=\varepsilon(k,\theta)I_{2\times2}+\sum_{\alpha=1}^{3}d_\alpha(k,\theta)\cdot\delta_\alpha$, and the unit vector $\hat{\boldsymbol{d}}$ are given by

$$\hat{\boldsymbol{d}}=\left\{\begin{array}{c}\frac{\left(1+\frac{1}{2}\cos[\theta]\right)+\cos[k]\left(1+t_3-\frac{1}{2}\cos[\theta]\right)}{\sqrt{\left(\left(1+\frac{1}{2}\cos[\theta]\right)+\cos[k]\left(1+t_3-\frac{1}{2}\cos[\theta]\right)\right)^2+\left(1-t_3-\frac{1}{2}\cos[\theta]\right)^2\sin[k]^2+\cos[k]^2(2h-2\sin[\theta]\sin[\varphi])^2}}\\ \frac{\left(1-t_3-\frac{1}{2}\cos[\theta]\right)\sin[k]}{\sqrt{\left(\left(1+\frac{1}{2}\cos[\theta]\right)+\cos[k]\left(1+t_3-\frac{1}{2}\cos[\theta]\right)\right)^2+\left(1-t_3-\frac{1}{2}\cos[\theta]\right)^2\sin[k]^2+\cos[k]^2(2h-2\sin[\theta]\sin[\varphi])^2}}\\ \frac{\cos[k](2h-2\sin[\theta]\sin[\varphi])}{\sqrt{\left(\left(1+\frac{1}{2}\cos[\theta]\right)+\cos[k]\left(1+t_3-\frac{1}{2}\cos[\theta]\right)\right)^2+\left(1-t_3-\frac{1}{2}\cos[\theta]\right)^2\sin[k]^2+\cos[k]^2(2h-2\sin[\theta]\sin[\varphi])^2}}\end{array}\right\}.$$

Then substituting unit vector $\hat{\boldsymbol{d}}$ into Berry curvature $F_{\mu\nu}=\frac{1}{2}[\hat{\boldsymbol{d}}\cdot\partial_\mu\hat{\boldsymbol{d}}\times\partial_\nu\hat{\boldsymbol{d}}]$, we can obtain $F_{k\theta}=$

$$\frac{\begin{array}{l}\left(\cos[k]^2\left(-1+t_3+\frac{1}{2}\cos[\theta]\right)\left(\frac{1}{2}h\sin[\theta]-\left(\frac{1}{2}+\cos[\theta]\right)\sin[\varphi]\right)-\cos[k]^3\left(-1+t_3+\frac{1}{2}\cos[\theta]\right)\left(\frac{1}{2}h\sin[\theta]+\left(-\frac{1}{2}+(1+t_3)\cos[\theta]\right)\sin[\varphi]\right)\right.\\ \left.-\cos[k]\left(-1+t_3+\frac{1}{2}\cos[\theta]\right)\sin[k]^2\left(\frac{1}{2}h\sin[\theta]+\left(-\frac{1}{2}+(1+t_3)\cos[\theta]\right)\sin[\varphi]\right)+\frac{1}{2}(2-t_3)\sin[k]^2\sin[\theta](-h+\sin[\theta]\sin[\varphi])\right)\end{array}}{\left(\left(1+\frac{1}{2}\cos[\theta]+\cos[k]\left(1+t_3-\frac{1}{2}\cos[\theta]\right)\right)^2+\left(-1+t_3+\frac{1}{2}\cos[\theta]\right)^2\sin[k]^2+4\cos[k]^2(h-\sin[\theta]\sin[\varphi])^2\right)^{3/2}}.$$

Acknowledgements

Project supported by the Beijing Natural Science Foundation (Grant No. 1232026), the Qinxin Talents Program of BISTU (Grant No. QXTCP C201711), the R&D Program of Beijing Municipal Education Commission (Grant No. KM202011232017), the National Natural Science Foundation of China (Grant No. 12304190), and the Research fund of BISTU (Grant No. 2022XJJ32).

References

[1] Su W P, Schrieffer J R and Heeger A J 1979 *Phys. Rev. Lett.* **42** 1698
[2] Hasan M Z and Kane C L 2021 *Rev. Mod. Phys.* **82** 3045
[3] X L Qi and Zhang S C 2011 *Rev. Mod. Phys.* **83** 1057
[4] Bansil A, Lin H and Das T 2016 *Rev. Mod. Phys.* **88** 021004
[5] Witten E 2016 *Rev. Mod. Phys.* **88** 035001
[6] Li C F, Li X P and Wang L C 2018 *Europhys. Lett.* **124** 37003
[7] Chiu C K, *et al*. 2016 *Rev. Mod. Phys.* **88** 035005
[8] Kitaev A Y 2001 *Phys. Usp* **44** 131
[9] Haldane F D M 1988 *Phys. Rev. Lett.* **61** 2015
[10] Qi X L, Wu Y S and Zhang S C 2006 *Phys. Rev. B* **74** 085308
[11] Zak J 1989 *Phys. Rev. Lett.* **62** 2747
[12] Li X P, Zhao E H and Liu W V 2013 *Nat. Commun.* **4** 1523
[13] Delplace P, Ullmo D and Montambaux G 2011 *Phys. Rev. B* **84** 195452
[14] Ganeshan S, Sun K and Das S S 2013 *Phys. Rev. Lett.* **110** 180403
[15] Li L H, Xu Z H and Chen S 2014 *Phys. Rev. B* **89** 085111
[16] Takayama H, Lin-Liu Y R and Maki K 1980 *Phys. Rev. B* **21** 2388
[17] Su W P, Schrieffer J R and Heeger A J 1980 *Phys. Rev. B* **22** 2099
[18] Jackiw R and Rebbi C 1976 *Phys. Rev. D* **13** 3398
[19] Heeger A J, *et al*. 1988 *Rev. Mod. Phys.* **60** 781
[20] Ruostekoski J, Dunne G V and Javanainen J 2002 *Phys. Rev. Lett.* **88** 180401
[21] Li M, Pernice W H P and Tang H X 2009 *Nat. Photon.* **3** 464
[22] Weis S, *et al*. 2010 *Science* **330** 1520
[23] Lin, Q, *et al*. 2009 *Phys. Rev. Lett.* **103** 103601
[24] Xu X, *et al*. 2022 *Front. Phys.* **9** 813801
[25] Provost J and Vallee G 1980 *Communications in Mathematical Physics* **76** 289
[26] Ma Y Q, *et al*. 2010 *Phys. Rev. B* **81** 245129
[27] Sachdev S 1999 *Physics World* **12** 33
[28] Sondhi S L, Girvin S M and Carini J P and Shahar D 1997 *Rev. Mod. Phys.* **69** 315
[29] Vojta M 2003 *Rep. Prog. Phys.* **66** 2069
[30] Neupert T, Santos L, Chamon C and Mudry C 2011 *Phys. Rev. Lett.* **106** 236804
[31] Haldane F 2004 *Phys. Rev. Lett.* **93** 206602
[32] Rhim J W, Kim K and Yang B J 2020 *Nature* **584** 59
[33] Peotta S and Torma P 2015 *Nat. Commun.* **6** 8944
[34] Huhtinen K E, Herzog-Arbeitman J, Chew A, Bernevig B A and Torma P 2022 *Phys. Rev. B* **106** 014518
[35] Gao Y and Xiao D 2019 *Phys. Rev. Lett.* **122** 227402
[36] Lapa M F and Hughes T L 2019 *Phys. Rev. B* **99** 121111
[37] Kozii V, Avdoshkin A, Zhong S and Moore J E 2021 *Phys. Rev. Lett.* **126** 156602
[38] Mitscherling J and Holder T 2022 *Phys. Rev. B* **105** 085154
[39] Ahn J, Guo G Y, Nagaosa N, *et al*. 2022 *Nat. Phys.* **18** 290
[40] Chen W and Huang W 2021 *Phys. Rev. Res.* **3** L042018
[41] Titus Neupert, *et al*. 2013 *Phys. Rev. B* **87** 245103
[42] Ajit S and Imamolu A 2015 *Phys. Rev. Lett.* **115** 166802
[43] Albert V V, Bradlyn B, Fraas M, *et al*. 2016 *Phys. Rev. X* **6** 041031
[44] Tan X S, *et al*. 2019 *Phys. Rev. Lett.* **122** 210401
[45] Ahn J, Guo G Y and Nagaosa N 2020 *Phys. Rev. X* **10** 041041
[46] Tan X S, *et al*. 2021 *Phys. Rev. Lett.* **126** 017702
[47] Li Z, *et al*. 2021 *Sci. China Phys. Mechan. Astron.* **64** 107211
[48] Gonzalesz Diego, Daniel Gutirrez-Ruiz and J David Vergara 2020 *J. Phys. A: Math. Theor.* **53** 505305

[49] Bruno M, Zhang A W and Goldman N 2022 *SciPost Physics* **12** 018
[50] Zhu Y Q, *et al*. 2021 *Phys. Rev. B* **104** 205103
[51] Bhalla P, *et al*. 2021 *Phys. Rev. Lett.* **129** 227401
[52] Li Z, *et al.* 2021 arXiv:2110.11649
[53] Ding H T, *et al*. 2022 *Phys. Rev. A* **105** 012210
[54] Bruno M and Mitscherling J 2022 *Phys. Rev. B* **106** 165133
[55] Zhai D W, *et al*. 2023 *Nat. Commun.* **14** 1961
[56] Ma Y Q and Chen S 2009 *Phys. Rev. A* **79** 022116
[57] Yang L, Ma Y Q and Li X G 2015 *Physica B* **456** 359
[58] Ma Y Q, *et al*. 2013 *Europhys. Lett.* **103** 10008
[59] Kruchkov A 2022 arXiv:2210.00351
[60] Kruchkov A 2022 *Phys. Rev. B* **105** L241102
[61] Tan X S, *et al*. 2019 *Phys. Rev. Lett.* **122** 210401
[62] Ma Y Q, *et al*. 2013 *Phys. Lett. A* **377** 1250
[63] Molignini P, *et al*. 2021 *Phys. Rev. B* **103** 184507
[64] Chen W and Gero von Gersdorff 2022 arXiv:2202.03494
[65] von Gersdorff G and Chen W 2019 *Phys. Rev. B* **104** 195133
[66] Porlles D and Chen W 2023 arXiv:2306.07366
[67] Ma Y Q 2014 *Phys. Rev. E* **90** 042133
[68] Kolodrubetz M, *et al*. 2017 *Phys. Rep.* **697** 1
[69] Ma Y Q, *et al*. 2021 *Europhys. Lett.* **100** 60001
[70] de Sousa, Matheus S M, Antonio L C and Chen W 2023 arXiv:2301.06493
[71] Yi C R, *et al.* 2023 arXiv:2301.06090
[72] Chen W and von Gersdorff G 2022 *SciPost. Phys. Core* **5** 040
[73] Ma Y Q 2020 arXiv:2001.05946